Requirement of PPARα in maintaining phospholipid and triacylglycerol homeostasis during energy deprivation

Susanna S. T. Lee,[1,*] Wood-Yee Chan,[†] Cherry K. C. Lo,[*] David C. C. Wan,[*] David S. C. Tsang,[*] and Wing-Tai Cheung[*]

Department of Biochemistry* and Department of Anatomy,† The Chinese University of Hong Kong, Shatin, New Territories, Hong Kong, China

Abstract The peroxisome proliferator-activated receptor α (PPARα) has been implicated as a key control of fatty acid catabolism during the cellular fasting. However, little is known regarding changes of individual fatty acids in hepatic triacylglycerol (TG) and phospholipid (PL) as a result of starvation. In the present work, the effects of 72 h fasting on hepatic TG and PL fatty acid profiles in PPARα-null (KO) mice and their wild-type (WT) counterparts were investigated. Our results indicated that mice deficient in PPARα displayed hepatomegaly and hypoketonemia following 72 h starvation. Histochemical analyses revealed that severe fatty infiltration was observed in the livers of KO mice under fasted conditions. Furthermore, 72 h fasting resulted in a 2.8-fold higher accumulation of hepatic TG in KO mice than in WT mice fasted for the same length of time. Surprisingly, the total hepatic PL contents in fasted KO mice decreased by 45%, but no significant change in hepatic PL content was observed in WT mice following starvation. Gas chromatographic analysis indicated that KO mice were deprived of arachidonic (20:4n-6) and docosahexaenoic (22:6n-3) acids during fasting. Taken together, these results show that PPARα plays an important role in regulation of fatty acid metabolism as well as phospholipid homeostasis during energy deprivation.— Lee, S. S. T., W-Y. Chan, C. K. C. Lo, D. C. C. Wan, D. S. C. Tsang, and W-T. Cheung. **Requirement of PPARα in maintaining phospholipid and triacylglycerol homeostasis during energy deprivation. *J. Lipid Res.* 2004.** 45: **2025–2037.**

Supplementary key words adipose tissue • arachidonic acid • docosahexaenoic acid • fatty acid profiling • fatty liver • hepatomegaly • 3-hydroxy-3-methylglutaryl coenzyme A synthase • hypoketonemia • ketone bodies • peroxisome proliferator-activated receptor α • starvation

The regulation of lipid metabolism in higher organisms appears to be closely associated with the activities of the peroxisome proliferator-activated receptor (PPAR) family. PPAR belongs to the nuclear hormone receptor superfamily, which consists of a group of ligand-activated DNA transcription factors that bind regulatory sequences upstream of their target genes, resulting in the activation or repression of specific gene transcription (1, 2). So far, three PPAR subtypes including PPARα (3), PPARβ (4) [and its homologues δ (3)/NUC-1 (5) or fatty acid-activated receptor (6)], and PPARγ (7, 8) have been described in mouse (9, 10), frog (11), rat (12), and human (7, 13). A close examination of the target genes containing peroxisome proliferator responsive element (PPRE) suggests that PPARα plays a central role in fat metabolism, including breakdown (14), storage (15), synthesis (16), and transport (17).

Among the PPAR subtypes, PPARα has been identified as a key modulator of cellular levels of fatty acids by regulating their catabolism (18–20). It has been shown that fatty acids are used as metabolic fuels, as signaling molecules, and as essential components of cellular membranes. It is thus logical to hypothesize that fatty acid levels should be closely regulated, and PPARα should become increasingly important in modulation of fatty acid metabolism, transport, storage, and intracellular energy balance during periods of starvation in which fatty acids are delivered to the liver for metabolic fuels.

Definite proof that PPARα plays a significant role in regulation of lipid homeostasis comes from the several starvation studies with PPARα-null (KO) mice (21–26). In these studies, short-term fasting (12–72 h) in KO mice resulted in hepatic steatosis, myocardial lipid accumulation, hypoketonemia, and hypoglycemia and it altered some gene expressions. Results of these studies clearly show that PPARα plays a pivotal role in management of energy stores during fasting, a condition in which an increased requirement of hepatic fatty acid oxidation occurs.

It has been shown that fatty acids and eicosanoids are the endogenous ligands for PPAR (27, 28), and any changes in endogenous fatty acid profiles will modulate the activity of PPAR. Although previous studies clearly show that PPARα plays a central role in fatty acid homeostasis during energy

Manuscript received 24 February 2004 and in revised form 19 August 2004.

Published, JLR Papers in Press, September 1, 2004.
DOI 10.1194/jlr.M400078-JLR200

Abbreviations: KO, PPARα-null [knockout]; PL, phospholipid; WT, wild-type.

[1] To whom correspondence should be addressed.
e-mail: lee2022@cuhk.edu.hk

deprivation, information is lacking regarding changes in fatty acid profiles during activation of PPARα. Hence, the aim of the present study was to determine, by using a PPARα-deficient mouse line (i.e., a line lacking PPARα expression) (29), the PPARα-mediated changes in fatty acid profiles in liver during 72 h starvation, a pathophysiological condition associated with disturbances in fatty acid homeostasis. We observed a significant depletion of hepatic phospholipids (PL), but a significant accumulation of hepatic TGs, in starved KO mice, suggesting that PPARα is required in maintaining hepatic TG and PL homeostasis during fasting. Furthermore, depletion of arachidonic (20:4n-6) and docosahexaenoic (22:6n-3) acids was found in PPARα mice under fasted conditions. To our knowledge, this is the first report of changes in hepatic PL fatty acid profiles in mice deficient in PPARα during energy deprivation.

MATERIALS AND METHODS

Materials

Chloroform, diethyl ether, hexane, methanol, toluene, neutral red, and eosin were purchased from BDH Laboratory Supplies (Dorset, England). Permount was obtained from Fisher (Hampton, NH), and the optimal cutting temperature (OCT) compound was from Sakura Finetek (Tokyo, Japan). Mayer's hematoxylin was purchased from Polysciences (PA, USA). Formalin and paraformaldehyde were purchased from Riedel de Haën (Germany). Digoxigenin (DIG) DNA labeling kit, nitroblue tetrazolium chloride (NBT), and 5-bromo-4-chloro-3-indolyl phosphate (BCIP) were from Boehringer Mannheim (Roche Diagnostics, Mannheim, Germany). Boron trifluoride-methanol, 2′,7′-dichlorofluorescein in 95% methanol, L-α-phosphatidylcholine diheptadecanoyl, triheptadecanoin, fatty acid methyl ester standards, Sudan Black B (practical grade), and all other reagents of the highest grade available were purchased from Sigma-Aldrich (St. Louis, MO).

Animals

The KO mice and their WT counterparts are inbred strains on an Sv/129 genetic background (29). A pair of parental stocks of KO and WT mice was shipped from the U.S. National Cancer Institute (National Institutes of Health, Bethesda, MD). They were then bred and reared at the Chinese University of Hong Kong Laboratory Animal Service Unit on a 12 h light/dark cycle (light: 06:00–18:00 h). Animals were fed on Laboratory Diet™ brand mouse diet No. 5015 (PMI Nutrition, St. Louis, MO) and chlorinated tap water ad libitum.

Animal treatment

Male KO and their wild-type (WT) counterparts (20–30 g, 12 weeks old) were acclimatized for at least 1 week prior to the experiments. The WT and KO mice were starved for 72 h, during which time they were allowed free access to water. Controls for each group were fed with regular mouse chow diet. After 72 h, mice were weighed and sacrificed by decapitation. Blood was collected into 1.5 ml Eppendorf tubes and serum was obtained after the blood was allowed to clot at room temperature for 30 min, and centrifuged at 3,000 rpm for 20 min. The whole liver was excised, weighed, and a small section (~1 cm^3) was removed from the median lobe and fixed either in 10% formalin in PBS for histopathology examination or in 4% paraformaldehyde for lipid staining. The remaining liver lobes were snap-frozen, wrapped in aluminum foil, and stored in liquid nitrogen until used for RNA and lipid analyses. Immediately following removal of the liver, the kidney, heart, spleen, subscapular brown fat, and epididymal white fat pads were excised and weighed.

Serum β-hydroxybutyrate, TG, and cholesterol analyses

Serum β-hydroxybutyrate, a marker of ketone body formation, was measured using an enzymatic kit (No. 310A) obtained from Sigma-Aldrich. Similarly, serum TG and cholesterol levels were measured using commercial kits (No. 33740A and 33710B and 402-20, respectively) purchased from Sigma-Aldrich.

Liver histology

Small pieces (~1 cm^3) of liver tissue were excised from the median lobe of mice for liver histopathology analysis. Three liver samples were collected for each treatment group. The tissues were fixed in 10% phosphate-buffered formalin for 48 h and then transferred to 70% alcohol, processed and embedded in paraffin. Liver sections (5 μm thick) were cut and stained with Mayer's hematoxylin and eosin for histological examination under a light microscope.

Sudan Black staining for lipids

Intracellular lipids were stained according to procedures described previously (30), with modifications. After the animal was sacrificed, small pieces (~1 cm^3) of liver tissue were quickly taken and immediately fixed in 4% paraformaldehyde at 4°C overnight. The liver tissues were then soaked in 20% sucrose before they were processed and embedded in OCT compound for cryosectioning with a cryostat (Reichert Jung, Germany). The sections (10 μm thick) were stored at −20°C. The stained sections were then allowed to dry at room temperature for about 30 min before they were rinsed in 70% alcohol. The sections were then stained for 15 min in a saturated solution of Sudan Black in 70% alcohol. The saturated Sudan Black solution was filtered through a Whatman No. 1 paper before use. The excess staining solution was removed by rinsing the sections with 70% alcohol. The sections were counterstained with 1% neutral red for 5 min, washed in distilled water, and mounted in pure glycerol. Unsaturated cholesterol esters, TGs, and PLs were stained blue black. Photographs were taken immediately, because the counterstain tended to fade with time.

Periodic acid-Schiff staining for carbohydrates and glycogen

Tissue carbohydrates, particularly glycogen, were stained by the periodic acid-Schiff (PAS) reaction as described previously (31). Briefly, the Schiff's reagent was prepared by dissolving 1 g basic fuchsin in 200 ml of boiling distilled water. The solution was allowed to cool to 50°C and potassium metabisulfite (2 g) was added, with constant mixing, in a completely dark condition. The solution was then allowed to cool to room temperature and concentrated hydrochloric acid (2 ml) was added and mixed. The solution was allowed to stand overnight in the dark. Activated charcoal (0.2 g) was then added and shaken for 1–2 min. After filtering through a Whatman No. 1 filter paper, the solution became either clear or pale yellow. The solution was stable for 1 month when kept at 4°C. Paraffin sections (5 μm thick) were rehydrated in a series of graded alcohol and treated with 1% periodic acid for 2 min. The sections were washed with several changes of distilled water before stained with the Schiff's reagent under a completely dark condition for 8 min. The excess Schiff's reagent was removed by rinsing the sections with distilled water. The sections were counterstained with Mayer's hematoxylin for 1 min, washed with distilled water, dehydrated in a series of graded ethanol, and

then mounted with Permount. Periodate-reactive carbohydrates and glycogen were stained with a magenta color.

Hepatic lipid analysis

Lipid extraction. Total lipid was extracted from the mouse liver (~300 mg) as described previously (32). Briefly, 2 mg of L-α-phosphatidylcholine diheptadecanoyl (internal standard of PL) and 1 mg of triheptadecanoin (internal standard of TG) were added to each liver sample immediately before homogenization. Liver was homogenized in 15 ml of chloroform-methanol 2:1 (v/v) using a polytron (Model PT-MR 3000 from Kinematica, Switzerland) for 3 min. This lipid extract was washed with 3 ml of 0.9% NaCl, vortexed, and then centrifuged at 2,500 rpm using a Beckman centrifuge (Model GS-15R) equipped with an S4180 rotor for 5 min. The bottom organic layer containing the total lipid extract was either subjected to fatty acid analysis by gas chromatography as detailed in the following sections, or the total lipid extract was further separated into TG and PL fractions by TLC as described in the next section. Total lipid content was calculated by summation of individual fatty acid content after separation by gas chromatography and expressed as mg FA/g liver.

Thin-layer chromatography. Different classes of lipid (including PLs, monoglycerides, diglycerides, cholesterol, free fatty acids, TGs, and cholesterol esters) were separated by TLC. The total lipid extract was evaporated to dryness under a stream of nitrogen. Chloroform (200 μl) was then added to resuspend the lipid extract. An aliquot (100 μl) of resuspended lipid extract was applied onto a TLC plate (Model SIL G-25 UV_{254} from Macherey-Nagel, Germany) using a 50 μl capillary tube (Sigma-Aldrich), and pure PL and TG standards were run in parallel. The TLC plate was then developed in a solvent mixture of hexane-diethyl ether-acetic acid 80:20:1 (v/v/v) for 45 min, dried, and sprayed briefly with a thin layer of fluorescent dye (2′,7′-dichlorofluorescein in 95% methanol). Following air-drying, plates were viewed under ultraviolet light. The yellow spots on the TLC plate corresponding to TG and PL were scraped with a razor blade and collected into screw-capped Pyrex glass tubes for subsequent methylation.

Methylation of fatty acids. The fatty acids were converted into fatty acid methyl esters and dimethyl acetals as described previously (33). The scraped spots containing PL or TG were transmethylated with boron trifluoride-methanol. Briefly, 1 ml of toluene and 2 ml of boron trifluoride-methanol were added to each sample. The samples were heated in a heating block (Thermolyne, USA) at 90°C for 45 min and then cooled to room temperature. To each of the tubes, 5 ml of hexane and 1 ml of distilled water were added. The tubes were then mixed and centrifuged at 2,500 rpm using a Beckman centrifuge (Model GS-15R) equipped with an S4180 rotor for 5 min. The upper clear organic layer was transferred to a clean test tube and was then evaporated under a stream of nitrogen using a nitrogen evaporator (Organization Associates, USA). After evaporation, the PL and TG pellets were dissolved in 100 and 200 μl of hexane (AnalaR grade), respectively.

Gas chromatography. After methylation, the composition of fatty acid methyl esters in TG and PL was determined by gas chromatography (GC). The PL or TG extract was transferred to 2-ml clear crimp vials (Hewlett-Packard, USA) and sealed with caps (Hewlett-Packard). GC was performed on a Hewlett-Packard 6890 Series GC System equipped with a flame ionization detector and an INNOWax (Cross-Linked polyethylene glycol) capillary column (30 m × 0.32 mm × 0.5 μm; Hewlett-Packard, No. 19091N-213). Samples (3 μl) were injected by an autosampler and injections were run under a constant flow of 1.3 ml/min with nitrogen as a carrier gas. A timed protocol was initiated with an oven temperature of 150°C for 1 min and was then programmed to increase oven temperature at a rate of 15°C/min to 200°C. This temperature was held for 2 min, then heated up to 250°C at a rate of 2°C/min and held for 5 min. The temperatures of the inlet and detector were 220°C and 275°C, respectively.

Chromatographic data were acquired and processed with Hewlett-Packard Chemstation software. The hepatic PL and TG fatty acid profiles are reported according to the length of carbon chain; individual fatty acids are expressed as a percentage of the sum of the peak areas for all the fatty acids. Fatty acids were identified by comparison of the peak retention times with those of known standards for saturated fatty acid methyl esters (No. ME-10) and unsaturated fatty acid methyl esters (No. ME-14) obtained from Sigma-Aldrich. The quantities of individual fatty acids were estimated by comparing their peak areas with the internal standard, heptadecanoate.

Total RNA isolation and Northern blot analysis

Total RNA was isolated from the livers of WT and KO mice with Trizol reagent (Invitrogen, Carlsbad, CA) as described by the manufacturer. Following size separation in a 1% formaldehyde-agarose gel, total RNA (20 μg) was transferred to a positively charged nylon membrane (Amersham, USA) by an upward capillary transfer method with 10× standard saline citrate (SSC) buffer overnight. The membrane was baked for 2 h at 80°C to fix the RNA onto the membrane.

DIG-labeled cDNA probe was synthesized using a DIG DNA labeling kit from Boehringer Mannheim. Briefly, cDNA of 3-hydroxy-3-methylglutaryl CoA (HMG-CoA) synthase (460 bp) subcloned in pCRII-TOPO vector (Invitrogen) was digested with *Eco*RI overnight and separated in a 1.5% agarose gel. The agarose band containing the HMG-CoA synthase cDNA insert was excised and the DNA was recovered from the agarose gel with a Qiagen gel extraction kit (Qiagen, USA). Purified cDNA fragment (1–2 μg) was labeled by random prime labeling using the DIG DNA labeling kit according to the manufacturer's recommendation.

After prehybridization in 15 ml of DIG Easy Hyb solution (Boehringer Mannheim) at 42°C for 4 h, the membrane was hybridized in 15 ml of hybridization buffer containing DIG-labeled cDNA probe at 42°C overnight. The hybridized membrane was washed twice for 15 min in 2× SSC containing 0.1% SDS at room temperature, twice for 15 min in 0.5× SSC containing 0.1% SDS at 60°C, and then once for 5 min in a maleic buffer (0.1 M maleic acid, 0.15 M NaCl; pH 7.5, 0.3% Tween 20) at room temperature. To reveal the hybridized RNA, the nonspecific binding sites on the membrane were first blocked by incubating in 1× Blocking buffer (Boehringer Mannheim) with gentle shaking for 30 min at room temperature. The membrane was then incubated with a polyclonal antibody against digoxigenin (Fab fragment conjugated to alkaline phosphatase, 1:20,000 dilution) in 1× Blocking buffer at room temperature for 1 h. After washing with maleic buffer twice for 15 min and once for 5 min with detection buffer (0.1 M Tris-HCl; pH 9.5, 0.1 M NaCl, 50 mM $MgCl_2$), the hybridized RNA was visualized by incubating the membrane with alkaline phosphatase substrate NBT/BCIP mixture in detection buffer as suggested by the manufacturer.

Statistical analysis

Data are expressed as mean ± SD. Differences in treatment means for the two strains of mice were analyzed using SigmaStat Advisory Statistical Software (SigmaStat version 2.01; SPSS, Chicago, IL). Each set of data was first tested for normality and equal variances. When the data set distributed normally with equal variances, a standard two-way ANOVA followed by a Tukey test was used to determine the significance of two-factor interactions (genotype × treatment) and the significant differences between treatment groups. For the data set that did not distribute normally and/or with equal variances, a standard Student's *t*-test or Mann-Whitney rank sum test was performed where appropriate

to assess the differences in treatment means. Statistical significance was determined at a level of $P < 0.05$.

RESULTS

Hepatomegaly was developed in fasted KO mice

Following 72 h of fasting, the body weight of WT mice was reduced by 24%. A similar reduction (21%) of body weight was observed in the KO mice fasted for the same length of time (**Fig. 1**). Despite reduction in body weight, the liver weight of fasted KO mice was increased by 60%, whereas only a slight but significant decrease of liver weight was found in fasted WT mice (**Fig. 2**). Interestingly, 72 h fasting caused a slight increase in the heart weights but a marked decrease in the spleen weights in both WT and KO mice (Fig. 2). On the other hand, 72 h fasting resulted in no significant differences in kidney weights between the WT mice and mice that lack PPARα (Fig. 2).

Peripheral lipid mobilization was retarded in fasted KO mice

To compare the degree of peripheral fat mobilization from adipose tissues between WT and KO mice during fasting conditions, the wet weights of epididymal fat pads and subscapular brown fats were measured in all four groups of animals. Significant reductions of epididymal fat pad weights occurred in both WT (55%) and KO (19%) mice after 72 h fasting (Fig. 2). However, it was intriguing to note that the reduction of epididymal fat pad weights in KO mice was 36% less than that in the WT mice. Similar results were reported by Lee and coworkers (34).

In addition to white adipose tissues, differential mobilization of lipids from subscapular brown fats was also observed between WT and KO mice following starvation. Marked depletion of subscapular brown fats was observed in fasted WT mice (41%), but only a slight decrease (11%) was noted in fasted KO mice (Fig. 2). Taken together, these results suggest that mobilization of fat depots is retarded during starvation in mice that lack PPARα.

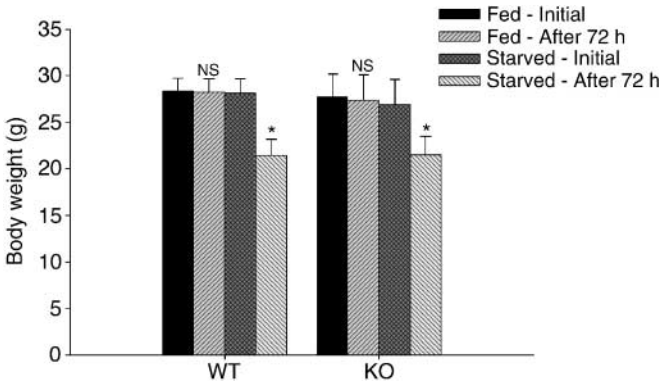

Fig. 1. Effect of 72 h starvation on body weights of wild-type (WT) and PPARα-null (KO) mice. WT and KO mice were randomly assigned to four treatment groups: WT-Fed ($n = 11$), WT-Starved ($n = 15$), KO-Fed ($n = 12$), and KO-Starved ($n = 12$). The mice were starved for 72 h; during this time they were allowed free access to water. Controls were fed with regular mouse chow diet. Data are expressed as mean ± SD. Two-way ANOVA indicates a statistically significant interaction between treatment and time ($P < 0.01$) for the same genotype, but no significant interaction between genotype and time for the same treatment, or between genotype and treatment for the same time point. * Significant difference with respect to genotype control according to a Tukey test following two-way ANOVA. NS, no significant difference.

Ketone body (β-hydroxybutyrate) production was dramatically reduced in fasted KO mice

To compare the ketotic states between WT mice and mice deficient in PPARα after 72 h of starvation, serum β-hydroxybutyrate, a measure of ketotic state was examined in these mice. Consistent with previous reports (22–25), a drastic increase (22.5-fold) of serum β-hydroxybutyrate levels was found in fasted WT mice (**Fig. 3**), but only a slight (2.6-fold) increase was detected in fasted KO mice. In line with the differential ketone body formation between WT and KO mice, expression of mitochondrial HMG-CoA synthase mRNA level, the key enzyme involved in ketone body formation, was markedly increased in WT but not in KO mice after 72 h starvation (**Fig. 4**). Note that the constitutive level of HMG-CoA synthase in KO mice was much lower than that in the WT control (Fig. 4), which is consistent with earlier report (35) that expression of HMG-CoA synthase is transcriptional regulated by PPARα.

In contrast to serum ketone body content, serum TG levels were decreased by 32% and 25% in fasted WT and KO mice, respectively (**Fig. 5**); this is in agreement with another report (24). Although there was a 38% increase of serum cholesterol level in WT mice, there was a 30% decrease in KO mice after 72 h fasting (**Fig. 6**). These data suggest that PPARα does not play a role in maintaining serum TG levels but may play an important role in regulation of serum cholesterol homeostasis during energy deprivation.

Fatty liver was induced in fasted KO mice

In addition to differences in liver weights between WT and KO mice following fasting, striking differences in liver color were also noted in these mice. Normal reddish-brown color was observed in the livers of both WT and KO mice under nonstarved conditions. Following 72 h of fasting, the color was changed to reddish orange and pale orange in the livers of WT and KO mice, respectively (data not shown). These observations suggest that fatty infiltration occurs in the livers of both WT and KO mice under fasted state, but the degree of fatty infiltration is more pronounced in mice that lack PPARα.

To assess whether fatty infiltration indeed occurred in the livers of WT and KO mice after 72 h starvation, gross liver histology, lipid-specific Sudan Black staining, and carbohydrate-specific PAS staining were performed on these livers. Our data revealed that WT mice under fed conditions (WT-Fed; $n = 3$) showed normal liver histology. Hepatocytes were arranged in a series of anastomosing plates, one cell thick, between which were sinusoidal spaces (**Fig. 7A**). These anastomosing plates extended from the periphery of a lobule to the central vein at its center in a ra-

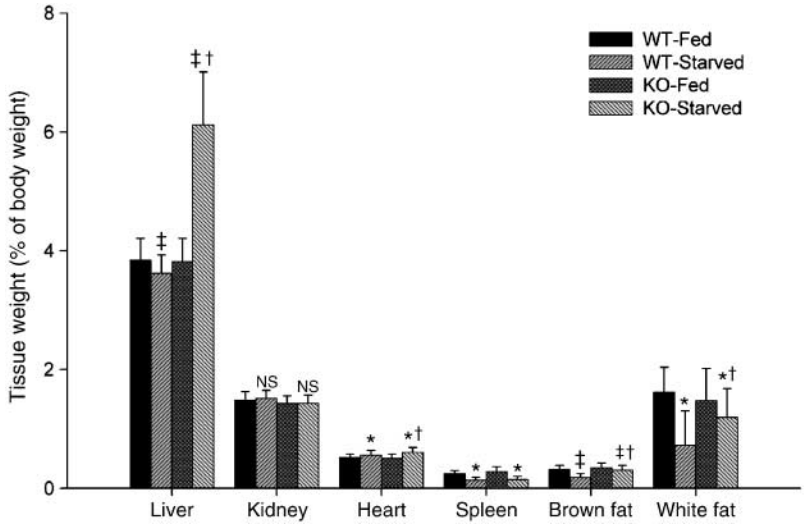

Fig. 2. Effect of 72 h starvation on organ weights of WT and KO mice. Following 72 h of starvation, mice were sacrificed and various organs were immediately removed and weighed. To account for change in body weight after starvation, the organ weights were normalized as percentage of body weight. Data are expressed as mean ± SD (n = 11–70). Two-way ANOVA indicates a statistically significant interaction between genotype and treatment in heart (P = 0.001) and white fat ($P < 0.001$). * Significant difference with respect to its genotype control according to a Tukey test following two-way ANOVA. ‡ Significant difference with respect to its genotype control by Student's t-test or Mann-Whitney rank sum test where appropriate. † Significant difference with respect to its treatment control by the corresponding statistical method used for genotype control analysis. NS, no significant difference.

dial fashion. The hepatocytes were polygonal, and the nuclei were vesicular in type with prominent and scattered chromatin. Lipid accumulation was not found in the hepatocytes, as indicated by weak reactivity to Sudan Black staining (**Fig. 8A**). Glycogen granules with positive PAS staining were found scattered throughout the cytoplasm of the hepatocytes (**Fig. 9A**). Similarly, livers of KO mice under nonstarved conditions (KO-Fed; n = 3) were also histologically normal (Fig. 7B). Normal arrays of anastomosing plates of polygonal hepatocytes extending radially from the periphery of a lobule to the central vein were found between sinusoidal spaces. Prominent hepatocyte nuclei with scattered chromatin were also noted. Sudan Black staining revealed that the lipid content in fed KO mice (Fig. 8B) was comparable to that found in the fed WT mice (Fig. 8A). In agreement with Kersten and coworkers (22), PAS staining revealed a lower cellular glycogen contents in fed KO mice (Fig. 9B) than in fed WT mice (Fig. 9A).

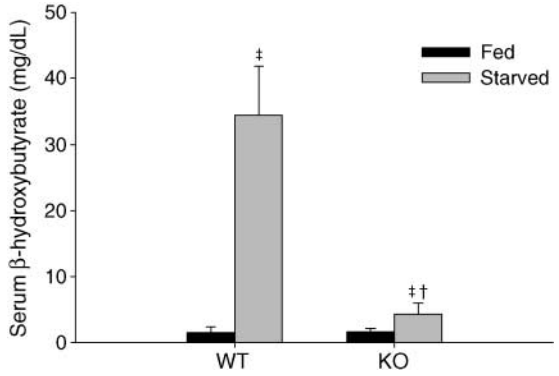

Fig. 3. Effect of 72 h starvation on serum β-hydroxybutyrate levels of WT and KO mice. Blood serum was collected from WT-Fed (n = 28), WT-Starved (n = 26), KO-Fed (n = 22), and KO-Starved (n = 23) mice after 72 h fasting and the serum β-hydroxybutyrate levels of these mice were determined as described in Materials and Methods. Data are expressed as mean ± SD. ‡ Significant difference with respect to its genotype control by Mann-Whitney rank sum test. † Significant difference with respect to its treatment control by the corresponding statistical method used for genotype control analysis.

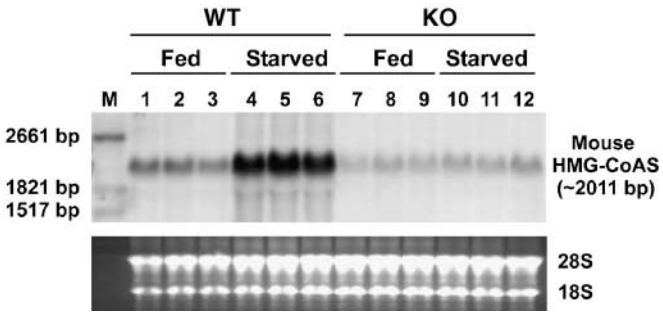

Fig. 4. Effect of 72 h starvation on hepatic HMG-CoA synthase expression levels of WT and KO mice. Total RNA (20 μg) was prepared from the livers of the four groups of animals (n = 3 per treatment group) following 72 h starvation. After size-separation by formaldehyde-agarose gel electrophoresis, RNA was transferred to a nylon membrane and hybridized with a digoxigenin-labeled HMG-CoA synthase probe as described in Materials and Methods. The intensity of 28S and 18S in the ethidium bromide-stained agarose gel indicates that approximate equal amounts of total RNA were loaded, and each lane represents an RNA sample from an individual mouse. Data shown are representative of two separate experiments with similar results.

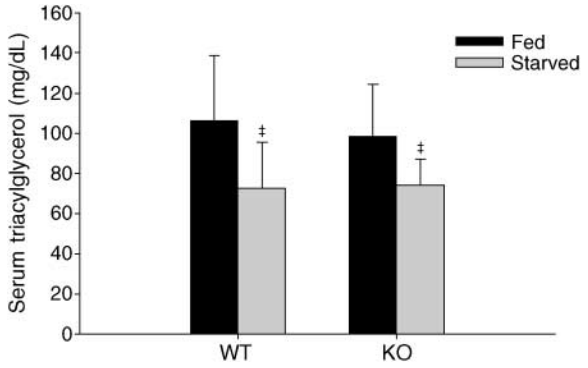

Fig. 5. Effect of 72 h starvation on serum triacylglycerol (TG) levels of WT and KO mice. After 72 h of fasting, blood serum was collected from WT-Fed ($n = 28$), WT-Starved ($n = 26$), KO-Fed ($n = 22$), and KO-Starved ($n = 23$) mice and the serum TG levels of these mice were determined as described in Materials and Methods. Data are expressed as mean ± SD. ‡ Significant difference with respect to its genotype control by Mann-Whitney rank sum test.

When the WT or KO mice were subjected to 72 h of fasting, the liver histology appeared to be changed. In WT mice starved for 72 h (WT-Starved; $n = 3$), although hepatocytes were found to maintain their normal anastomosing pattern, the sinusoidal spaces seemed to be less obvious and blood accumulation was found in most of the central veins (Fig. 7C). Many hepatocytes were moderately pleomorphic and foamy in appearance from microvesicular droplets accumulated inside the cytoplasm. When stained with Sudan Black for lipids, those microvesicular droplets appeared positive (Fig. 8C), indicating that the droplets contained lipids. PAS staining revealed that the number of glycogen granules was drastically reduced (Fig. 9C) as the animals were fasted, although positive granules

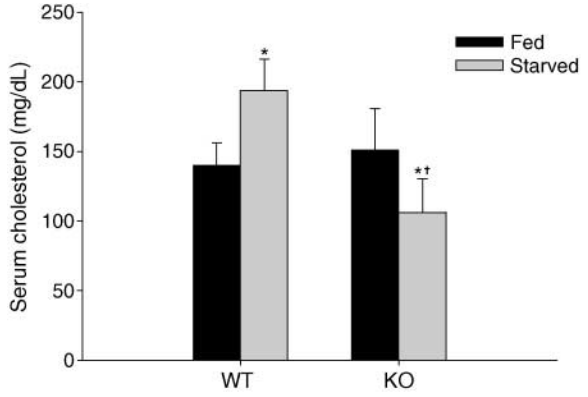

Fig. 6. Effect of 72 h starvation on serum cholesterol levels of WT and KO mice. Blood serum was collected from WT-Fed ($n = 28$), WT-Starved ($n = 26$), KO-Fed ($n = 22$), and KO-Starved ($n = 23$) mice following 72 h starvation and the serum cholesterol levels of these mice were determined as described in Materials and Methods. Data are expressed as mean ± SD. Two-way ANOVA indicates a statistically significant interaction between genotype and treatment ($P < 0.001$). * Significant difference with respect to its genotype control according to a Tukey test following two-way ANOVA. † Significant difference with respect to its treatment control by the corresponding statistical method used for genotype control analysis.

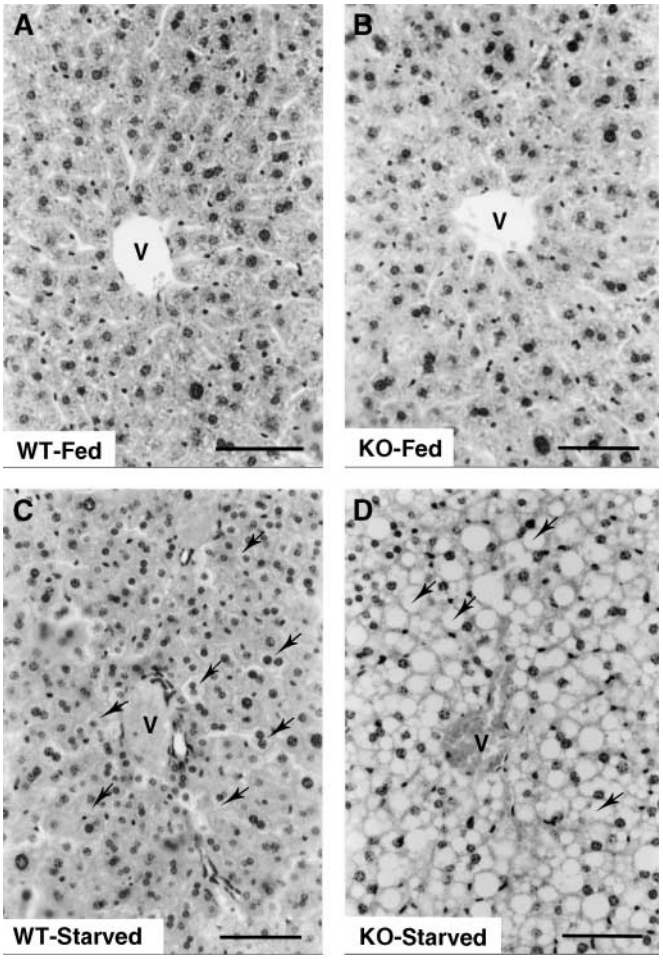

Fig. 7. Hematoxylin and eosin staining of WT and KO liver sections. Photomicrographs of paraffin sections (5 μm thick) taken from livers of (A) WT mice under fed conditions (WT-Fed; $n = 3$); (B) PPARα-null mice under fed conditions (KO-Fed; $n = 3$); (C) WT mice fasted for 72 h (WT-Starved; $n = 3$); and (D) PPARα-null mice fasted for 72 h (KO-Starved; $n = 3$). Normal liver histology was found in both WT and KO mice under nonstarved state (WT-Fed and KO-Fed). Polygonal hepatocytes were arranged in one-cell thick anastomosing plates, which extend radially from the periphery of a lobule to the central vein. Sinusoidal spaces were found between the anastomosing plates and scattered chromatin was seen inside the prominent nuclei. The fasted WT mice (WT-Starved), however, showed slightly collapsed sinusoidal spaces. Most of the central veins were congested with blood. Hepatocytes were moderately pleomorphic and foamy in appearance as numerous microvesicular droplets (arrows) were formed inside their cytoplasm. In fasted KO mice (KO-Starved), fatty changes in the liver were even more evident. The anastomosing plates were disarrayed and blood was accumulated in the central vein. Macrovesicular droplets (arrows), which were formed inside the hepatocyte cytoplasm compress and displace the nuclei to the periphery of the hepatocytes. Micrographs are representative of the treatment groups, and all three mice in the same treatment group show similar features. V, central vein. Bars, 50 μm.

could still be occasionally found in some hepatocytes. When KO mice were fasted for 72 h (KO-Starved; $n = 3$), the histological changes were even more dramatic (Fig. 7D). The anastomosing plates were disarrayed, with blood accumulated in the central veins. Apart from the forma-

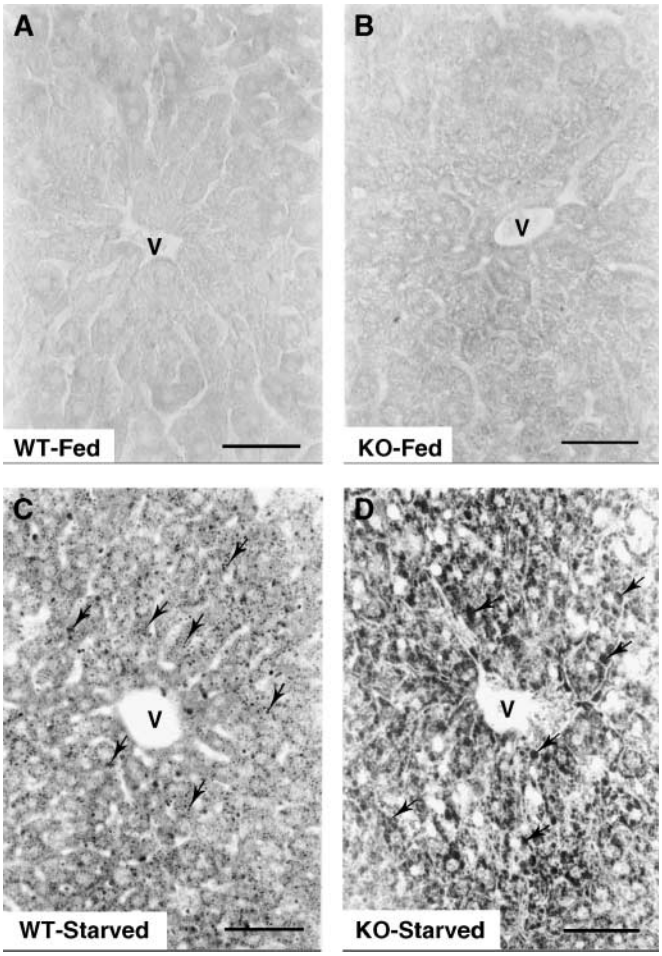

Fig. 8. Sudan Black staining for lipids in WT and KO liver sections. Photomicrographs of frozen sections (10 μm thick) taken from livers of (A) WT mice under fed conditions (WT-Fed; $n = 3$); (B) PPARα-null mice under fed conditions (KO-Fed; $n = 3$); (C) WT mice fasted for 72 h (WT-Starved; $n = 3$); and (D) PPARα-null mice fasted for 72 h (KO-Starved; $n = 3$). All sections were stained with Sudan Black staining for lipids. A very weak reactivity was found in almost all the hepatocytes of WT and KO mice under nonstarved conditions (WT-Fed and KO-Fed). In fasted WT mice (WT-Starved), positive staining (arrows) was found in the microvesicular droplets inside the cytoplasm of the hepatocytes, indicating that the droplets contain lipids. In fasted KO mice (KO-Starved), both the microvesicular and macrovesicular droplets (arrows) were strongly stained. Micrographs are representative of the treatment groups, and all three mice in the same treatment group show similar features. V, central vein. Bars, 50 μm.

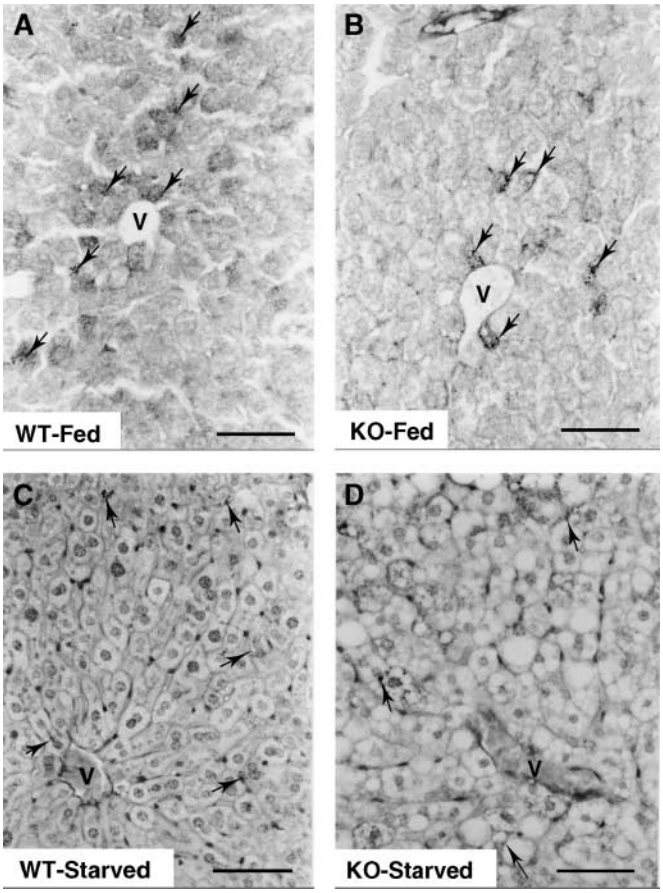

Fig. 9. Periodic acid-Schiff staining for glycogen in WT and KO liver sections. Photomicrographs of paraffin sections (5 μm thick) taken from livers of (A) WT mice under fed conditions (WT-Fed; $n = 3$); (B) PPARα-null mice under fed conditions (KO-Fed; $n = 3$); (C) WT mice fasted for 72 h (WT-Starved; $n = 3$); and (D) PPARα-null mice fasted for 72 h (KO-Starved; $n = 3$). All sections were stained with periodic acid-Schiff staining for glycogen and periodate-reactive carbohydrates. In both WT and KO mice under nonstarved conditions (WT-Fed and KO-Fed), positive glycogen granules (arrows) were found in the hepatocytes, but the number of the glycogen granules (arrows) were drastically depleted in the hepatocytes of both fasted WT (WT-Starved) and fasted KO (KO-Starved) mice. Micrographs are representative of the treatment groups, and all three mice in the same treatment group show similar features. V, central vein. Bars, 50 μm.

tion of the microvesicular droplets, large macrovesicular droplets were also found inside the cytoplasm of hepatocytes, compressing and displacing the nucleus to the periphery of the hepatocytes. The strong positive reactions to Sudan Black staining indicated that both the microvesicular and macrovesicular droplets contained lipids (Fig. 8D). The PAS staining also showed a marked depletion of the glycogen granules in the hepatocytes of starved KO mice (Fig. 9D) compared with KO mice under nonstarved conditions. A similar reduction in glycogen granules was also found in WT mice fasted for the same length of time (Fig. 9C). Taken together, these findings show that depletion of PPARα leads to a substantial increase in lipid accumulation in the liver during fasting.

Hepatic TG was increased and PL was decreased in fasted KO mice

To more accurately quantitate the differences in lipid accumulation in livers of WT and KO mice under fasting conditions, we measured the total lipid contents in the livers of these mice by gas chromatographic separation of the fatty acid methyl esters derived from their hepatic lipid extracts. Following 72 h of starvation, the hepatic total lipid contents (mg FA/g liver) were significantly increased by 4.4- and 8-fold in WT and KO mice, respectively (**Fig. 10A**). The 4-fold increase in hepatic lipid contents in WT mice is similar to the findings of others (26, 36). The ob-

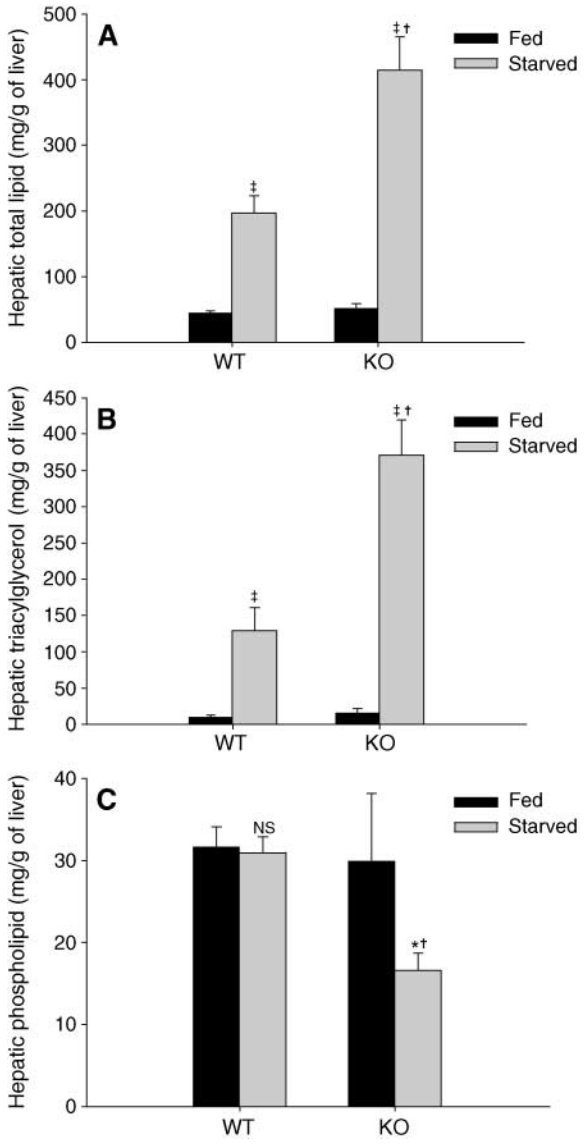

Fig. 10. Effect of 72 h starvation on hepatic lipid contents of WT and KO mice. Total lipids were extracted from the livers of WT ($n = 5$ per treatment group) and KO ($n = 5$ per treatment group) mice under fed or starved conditions. Phospholipid (PL) and triacylglycerol (TG) were separated from the total lipid extract by TLC. Fatty acids from the total lipid extract, TG, and PL were converted into methyl esters and the fatty acid methyl esters were then separated by gas chromatography as described in Materials and Methods. Levels (mg FA/g liver) of hepatic total lipid (A), TG (B) and PL (C) were obtained by summation of the individual fatty acids derived from total hepatic lipid, TG and PL, respectively. Data are expressed as mean ± SD. Two-way ANOVA indicates a statistically significant interaction between genotype and treatment for hepatic PLs ($P = 0.007$). * Significant difference with respect to its genotype control according to a Tukey test following two-way ANOVA. ‡ Significant difference with respect to its genotype control by Student's *t*-test or Mann-Whitney rank sum test where appropriate. † Significant difference with respect to its treatment control by the corresponding statistical method used for genotype control analysis. NS, no significant difference.

servation that substantially higher amounts of hepatic lipids were detected in fasted KO mice further supported the morphological and histochemical data showing that more lipid droplets were formed in the hepatocytes of KO mice under fasted conditions (Fig. 8).

To reveal whether the increased hepatic total lipid contents in both WT and KO mice after 72 h fasting was due to an increase in TG and/or PL levels in these mice, their hepatic total lipid extracts were further separated into TG and PL by TLC and then followed by gas chromatographic analysis. Our results indicated that, in fasted WT mice, the increased hepatic total lipid contents resulted from a significant increase (12.3-fold) in TG levels only; the PL contents did not change (Fig. 10, panels B and C). Unlike the fasted WT mice, the increased hepatic lipid contents in fasted KO mice resulted from a significant increase in TG contents (23.5-fold) and a significant decrease (45%) in PL levels (Fig. 10, panels B and C). The 2.8-fold higher hepatic TG levels found in fasted KO mice compared with fasted WT mice are consistent with a previous report (24). Thus, these data indicate that a partial block in metabolism of TG and/or a defect in TG lipolysis occur in mice deficient in PPARα during starvation. Furthermore, a significant decrease in PL contents in KO mice suggests that PPARα may be involved in maintaining the integrity of PL membranes in the liver during energy deprivation.

Arachidonic and docosahexaenoic acids of hepatic TG and PL were depleted in fasted KO mice

To identify which fatty acids were depleted in hepatic PL in KO mice after 72 h fasting, the fatty acid profiles of hepatic PLs were examined. In WT mice under nonstarved conditions, 10 fatty acids were detected in the gas chromatogram. The relative contents of these fatty acids (% of total FA) were, in decreasing concentrations: palmitic (16:0; 23.02 ± 0.70%), linoleic (18:2n-6; 18.76 ± 0.64%), stearic (18:0; 17.80 ± 0.52%), arachidonic (20:4n-6; 15.70 ± 0.93%), docosahexaenoic (22:6n-3; 13.80 ± 0.87%), oleic (18:1n-9; 6.45 ± 0.51%), *cis*-vaccenic (18:1n-7; 1.65 ± 0.15%), bishomo-γ-linolenic (20:3n-6; 1.22 ± 0.68%), palmitoleic (16:1n-7; 0.70 ± 0.12%), and eicosapentaenoic (20:5n-3; 0.31 ± 0.42%) acids. The levels (mg/g liver) of these fatty acids, except for bishomo-γ-linolenic (20:3n-6) acid, were not significantly altered in WT mice following fasting (**Table 1**; **Fig. 11**). Strikingly, a selective depletion of eight fatty acids [palmitic (16:0), stearic (18:0), *cis*-vaccenic (18:1n-7), linoleic (18:2n-6), bishomo-γ-linolenic (20:3n-6), arachidonic (20:4n-6), eicosapentaenoic (20:5n-3), and docosahexaenoic (22:6n-3) acids] was observed in KO mice as a result of starvation (Table 1; Fig. 11).

Unlike the hepatic PL, 11 hepatic TG fatty acids were identified in the livers of WT and KO mice. In WT mice under fed conditions, the relative contents (% of total FA) of these fatty acids were, in decreasing concentrations: linoleic (18:2n-6; 31.13 ± 1.59%), oleic (18:1n-9; 26.18 ± 0.82%), palmitic (16:0; 24.16 ± 0.28%), docosahexaenoic (22:6n-3; 4.30 ± 0.88%), stearic (18:0; 3.88 ± 0.94%), palmitoleic (16:1n-7; 2.85 ± 0.43%), *cis*-vaccenic (18:1n-7; 2.54 ± 0.21%), α-linolenic (18:3n-3; 1.50 ± 0.20%), arachidonic (20:4n-6; 1.48 ± 0.22%), myristic (14:0; 0.84 ± 0.12%), and 16:1n-9 (0.67 ± 0.10%) acids. When the WT mice were fasted for 72 h, the contents (mg/g liver) of all

TABLE 1. Effect of 72 h starvation on hepatic PL fatty acid profiles of WT and KO mice

	Weight of FA (mg/g of Liver)			
	WT		KO	
Fatty Acids	Control	Starved	Control	Starved
14:0 (Myristic acid)	ND	0.02 ± 0.03	ND	0.04 ± 0.03
16:0 (Palmitic acid)	7.34 ± 0.63	7.28 ± 0.43	6.09 ± 1.75	3.17 ± 0.44
16:1n-9	ND	ND	ND	ND
16:1n-7 (Palmitoleic acid)	0.22 ± 0.05	0.25 ± 0.04	0.21 ± 0.06	0.24 ± 0.05
18:0 (Stearic acid)	5.67 ± 0.45	5.31 ± 0.36	6.01 ± 1.57	3.52 ± 0.51
18:1n-9 (Oleic acid)	2.05 ± 0.03	2.04 ± 0.10	1.80 ± 0.48	1.67 ± 0.27
18:1n-7 (*cis*-Vaccenic acid)	0.53 ± 0.07	0.43 ± 0.07	0.47 ± 0.14	0.22 ± 0.03
18:2n-6 (Linoleic acid)	5.98 ± 0.42	5.69 ± 0.32	6.54 ± 1.68	4.95 ± 0.61
18:3n-3 (α-Linolenic acid)	ND	ND	ND	ND
20:1n-11 (Gadoleic acid)	ND	ND	ND	ND
20:3n-6 (Bishomo-γ-linolenic acid)	0.40 ± 0.23	0.10 ± 0.22	0.33 ± 0.11	ND
20:4n-6 (Arachidonic acid)	5.01 ± 0.51	4.89 ± 0.42	4.81 ± 1.39	1.80 ± 0.23
20:5n-3 (Eicosapentaenoic acid)	0.10 ± 0.14	0.06 ± 0.13	0.34 ± 0.11	ND
22:5n-3 (Timnodonic acid)	ND	ND	ND	ND
22:6n-3 (Docosahexaenoic acid)	4.39 ± 0.24	4.87 ± 0.35	3.30 ± 0.97	0.95 ± 0.15

KO, PPARα-null; ND, not detectable; WT, wild type. Fatty acids were analyzed by gas chromatography as described in Materials and Methods. Data are expressed as mean ± SD ($n = 5$ for each group). Statistical analyses were performed with two-way ANOVA, Mann-Whitney rank sum test, or Student's *t*-test where appropriate. Significant differences ($P < 0.05$) are indicated in Fig. 11.

these fatty acids were significantly increased (**Table 2**; **Fig. 12**). In contrast, 72 h fasting caused accumulation of long chain (C14–18) fatty acids in larger amounts, whereas the levels of very long chain fatty acids (C20–24), including arachidonic (20:4n-6) and docosahexaenoic (22:6n-3) acids, were depleted to an undetectable level in KO mice under fasted conditions (Table 2; Fig. 12).

DISCUSSION

We show that PPARα is a physiological regulator in maintaining the TG as well as PL homeostasis under energy deprivation. Following 72 h of fasting, we observed a significant increase in liver weight and hepatomegaly in mice deficient in PPARα. Histochemical examination of liver cells revealed that fasting caused a marked accumulation of lipid droplets in KO mice. These observations were further substantiated by the gas chromatographic data showing that liver TG contents were increased by 2.8-fold in KO mice compared with the WT mice as a result of starvation. Taken together, these data suggest that PPARα is a key modulator of fatty acid metabolism in liver under fasted conditions, and the results are consistent with previous findings that activation of PPARα induces the expression of enzymes for fatty acid metabolism (37, 38). However, the molecular mechanism that leads to hepatomegaly and hepatic lipid accumulation is still an open question.

It is known that mobilization of fatty acids from adipose tissues occurs during short-term starvation, and fatty acid mobilization from adipose tissues occurred in both WT and KO mice during fasting. However, a slower reduction of adipose tissue weight was found in KO mice than in WT mice, suggesting that PPARα is involved in controlling TG mobilization from adipose tissues. Expression of PPARα was detected in brown adipose tissue, but PPARβ and PPARγ are the predominant isoforms detected in adipose tissues (19). Hence, the role of PPARα in adipose tissue lipid mobilization remains to be determined.

Under fasted conditions, a slight but consistent increase in heart weights was observed in both WT and KO mice; the increase was higher in KO than in the WT mice. It has been reported that lipoprotein lipase activity is increased in heart after fasting (39). Based on these different observations, it is tempting to speculate that the increased heart weight in KO mice may be due to accumulation of fatty acids in heart resulting from an increased cardiac lipoprotein lipase activity during starvation. Thus, it appears that expression of PPARα in heart (3) may be important for regulating cardiac fatty acid metabolism.

In addition to liver and heart, high expression of PPARα is also detected in kidney (3, 19). In the present study, we did not observe any significant changes in kidney weights between WT and KO mice under fasted conditions. These results suggest that PPARα-mediated increase of fatty acid metabolism is not a predominant energy-production pathway in this organ; however, the physiological roles of PPARα in kidney are unclear.

During fasting, ketone bodies generated by liver serve as alternative substrates of oxidation. It is known that HMG-CoA synthase, a mitochondrial enzyme, catalyzes the production of ketone bodies from long chain fatty acid during fasting. As expected, substantial accumulation of ketone bodies were found in the serum of fasted WT mice, as reflected by the remarkable high expression level of HMG-CoA synthase detected in these mice. By contrast, extremely low levels of ketone bodies were observed in mice deficient in PPARα. This is further supported by the observation that no significant induction of mitochondrial HMG-CoA synthase was measured in KO mice during starvation. The lack of HMG-CoA synthase induction in PPARα-deficient mice suggests that transcriptional activation of HMG-CoA synthase is dependent on the presence of PPARα under fasted state. This is in agreement with earlier findings

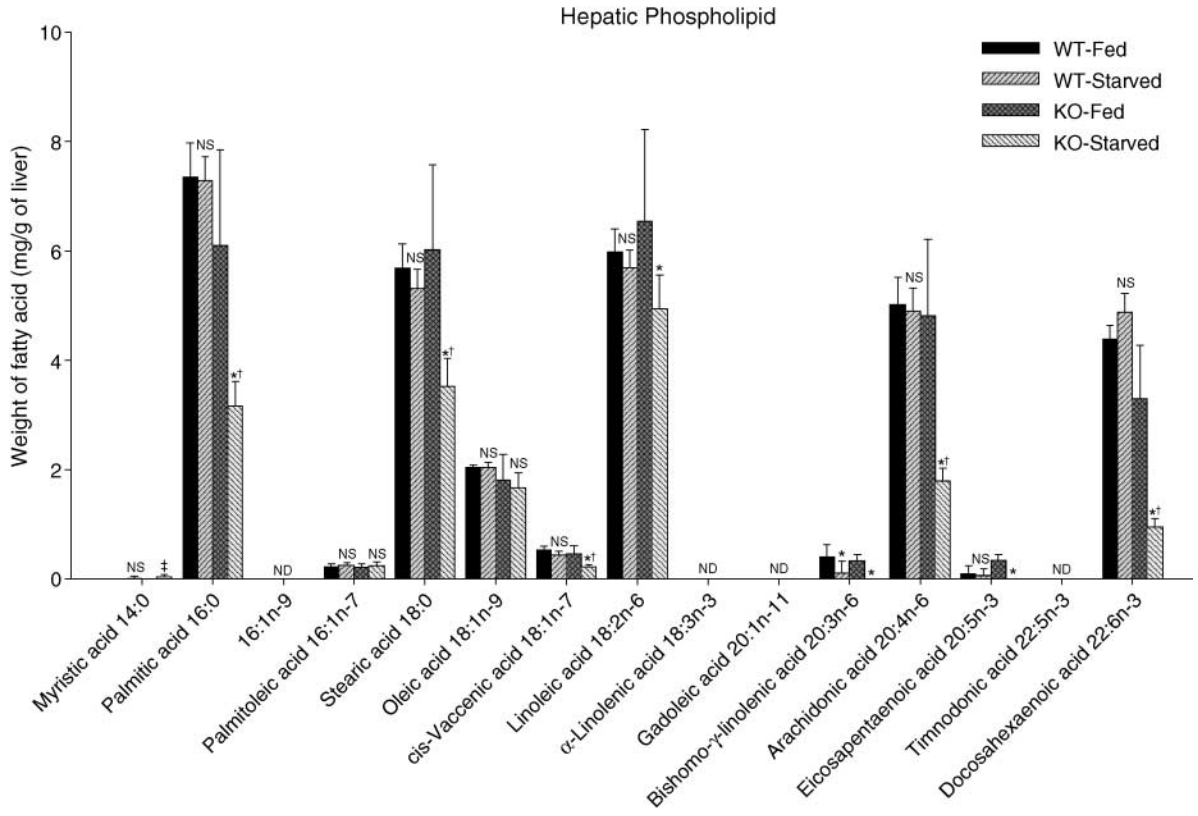

Fig. 11. Effect of 72 h starvation on hepatic PL fatty acid profiles of WT and KO mice. Total lipids were extracted from the livers of WT ($n = 5$ per treatment group) and KO ($n = 5$ per treatment group) mice under fed or starved conditions. PLs were separated from the total lipids by TLC. After conversion into methyl esters, fatty acids were separated by gas chromatography as described in Materials and Methods. Levels of individual fatty acids are expressed as mg FA/g liver. Data are expressed as mean ± SD. Two-way ANOVA indicates a statistically significant interaction between genotype and treatment for palmitic ($P = 0.005$), stearic ($P = 0.03$), arachidonic ($P < 0.001$), eicosapentaenoic ($P = 0.007$), and docosahexaenoic ($P < 0.001$) acids. * Significant difference with respect to its genotype control according to a Tukey test following two-way ANOVA. ‡ Significant difference with respect to its genotype control by Student's *t*-test or Mann-Whitney rank sum test where appropriate. † Significant difference with respect to its treatment control by the corresponding statistical method used for genotype control analysis. NS, no significant difference; ND, not detectable.

that a conserved PPRE is present in the promoter region of mitochondrial HMG-CoA synthase (16, 35). Thus, these data show that PPARα is the major factor required for production of ketone bodies during starvation.

A reduction of serum TG levels by 32% and 25% was observed in WT and KO mice, respectively, following 72 h of fasting. The reduction of serum TG level agreed with a previous finding that hepatocytes from fasted rats secrete smaller very low density lipoprotein (VLDL) and lesser amounts of TG than hepatocytes from fed control rats (40). No significant differences were found in serum total cholesterol levels between WT and KO mice under fed conditions. When the mice were subjected to 72 h of starvation, the serum total cholesterol level was increased by 38% in WT but decreased by 30% in KO mice. It has been reported that fasting selectively increases the secretion of apoE but decreases the secretion of low molecular weight apoB (40, 41). Furthermore, activation of PPARα in macrophages has been shown to upregulate the expression of class B scavenger receptors SR-B1 and CLA-1, which bind HDLs (42), and to reduce cholesterol esterification in macrophages, resulting in an increased efflux of free cholesterol through transporter ABCA1, a member of the ATP-binding cassette-transporter family (43, 44). These results suggest that PPARα may play an important role in regulation of cholesterol homeostasis by modulating the turnover of lipoproteins and recycling of free cholesterol. However, the exact role of PPARα in regulating hepatic cholesterol metabolism remains to be determined.

We observed that fasting induced an accumulation of hepatic TG, which was composed mainly of long chain (C14–18) fatty acids. The accumulation of these long chain fatty acids was more evident in mice deficient in PPARα. Moreover, a noticeable increase of very long chain (C20–24) fatty acids in hepatic TG, including arachidonic (20:4n-6) and docosahexaenoic (22:6n-3) acids, was observed in fasted WT mice, but the levels of these fatty acids were decreased to a nondetectable levels in fasted KO mice. Previous studies suggest a preferential mobilization of polyunsaturated fatty acids with carbon chain lengths of C18–22 from adipose tissue during fasting (45–47). Peroxisomes have been suggested to be specialized in β-oxidation of long chain fatty acids, and peroxisomal β-oxidation enzymes are induced via peroxisome proliferator-activated receptors (38, 48, 49). Taken together, these results suggest that the accumulated fatty acids in hepatic TG are derived from adi-

TABLE 2. Effect of 72 h starvation on hepatic TG fatty acid profiles of WT and KO mice

	Weight of FA (mg/g of Liver)			
	WT		KO	
Fatty Acids	Control	Starved	Control	Starved
14:0 (Myristic acid)	0.09 ± 0.02	1.07 ± 0.28	0.14 ± 0.07	5.27 ± 0.99
16:0 (Palmitic acid)	2.55 ± 0.41	23.96 ± 6.17	3.13 ± 1.11	68.35 ± 7.00
16:1n-9	0.07 ± 0.01	1.05 ± 0.32	0.10 ± 0.04	3.43 ± 0.52
16:1n-7 (Palmitoleic acid)	0.30 ± 0.09	4.06 ± 1.18	0.42 ± 0.27	21.54 ± 3.65
18:0 (Stearic acid)	0.41 ± 0.11	2.75 ± 0.79	0.57 ± 0.21	7.87 ± 0.53
18:1n-9 (Oleic acid)	2.76 ± 0.43	34.31 ± 8.94	3.74 ± 1.44	106.65 ± 7.13
18:1n-7 (*cis*-Vaccenic acid)	0.27 ± 0.06	2.35 ± 0.53	0.32 ± 0.10	8.57 ± 1.46
18:2n-6 (Linoleic acid)	3.29 ± 0.62	50.84 ± 12.18	5.59 ± 2.35	141.18 ± 26.96
18:3n-3 (α-Linolenic acid)	0.16 ± 0.04	2.14 ± 0.58	0.30 ± 0.15	7.99 ± 1.79
20:1n-11 (Gadoleic acid)	ND	ND	0.12 ± 0.09	ND
20:3n-6 (Bishomo-γ-linolenic acid)	ND	ND	0.04 ± 0.08	ND
20:4n-6 (Arachidonic acid)	0.15 ± 0.02	1.90 ± 0.48	0.24 ± 0.10	ND
20:5n-3 (Eicosapentaenoic acid)	ND	ND	0.08 ± 0.09	ND
22:5n-3 (Timnodonic acid)	ND	ND	0.09 ± 0.15	ND
22:6n-3 (Docosahexaenoic acid)	0.44 ± 0.06	4.37 ± 1.05	0.91 ± 0.33	ND

ND, not detectable. Fatty acids were analyzed by gas chromatography as described in Materials and Methods. Data are expressed as mean ± SD ($n = 5$ for each group). Statistical analyses were performed with two-way ANOVA, Mann-Whitney rank sum test, or Student's *t*-test where appropriate. Significant differences ($P < 0.05$) are indicated in Fig. 12.

pose tissues, and PPARα is required for effective utilization of long chain (C14–18) but not very long chain (C20–24) fatty acids in hepatic TG under fasting conditions.

Surprisingly, fasting induced a preferential depletion of palmitic (16:0), stearic (18:0), *cis*-vaccenic (18:1n-7), linoleic (18:2n-6), bishomo-γ-linolenic (20:3n-6), arachidonic (20:

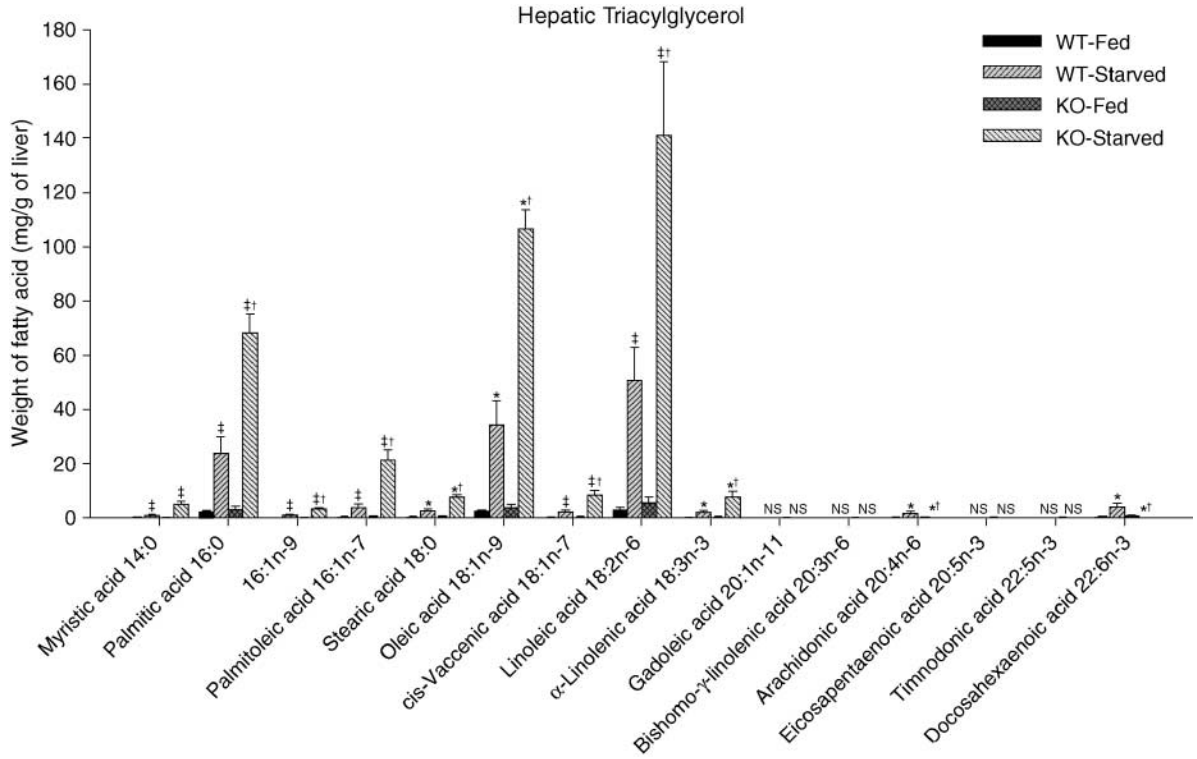

Fig. 12. Effect of 72 h starvation on hepatic TG fatty acid profiles of WT and KO mice. Total lipids were extracted from the livers of WT ($n = 5$ per treatment group) and KO ($n = 5$ per treatment group) mice under fed or starved conditions. Triacylglycerol (TG) was separated from the total lipid by TLC. After conversion into methyl esters, fatty acids were separated by gas chromatography as described in Materials and Methods. Levels of individual fatty acid are expressed as mg FA/g liver. Data are expressed as mean ± SD. Two-way ANOVA indicates a statistically significant interaction between genotype and treatment for stearic ($P < 0.001$), oleic ($P < 0.001$), α-linolenic ($P < 0.001$), arachidonic ($P < 0.001$) and docosahexaenoic ($P < 0.001$) acids. * Significant difference with respect to its genotype control according to a Tukey test following two-way ANOVA. ‡ Significant difference with respect to its genotype control by Student's *t*-test or Mann-Whitney rank sum test where appropriate. † Significant difference with respect to its treatment control by the corresponding statistical method used for genotype control analysis. NS, no significant difference.

4n-6), eicosapentaenoic (20:5n-3), and docosahexaenoic (22:6n-3) acids in KO mice but without any significant effects on the levels of these fatty acids, except for bishomo-γ-linolenic, in WT mice. The lack of significant changes in PL fatty acid contents in WT mice after 72 h fasting is in accord with previous report that fasting does not affect PL composition (50). Since both saturated and polyunsaturated fatty acids in PLs were depleted to a similar extent, we hypothesize that PPARα-deficient mice mobilize PLs during energy deprivation while sparing the fatty acids in TGs. It has been reported that intracellular levels of ATP were reduced by 52% and levels of cytosolic calcium ions were increased by 79% in hepatocytes isolated from fasted rats compared with the fed control (51). A calcium-activated, heparin-released phospholipase A1 (hepatic lipase) was identified in rat liver (52, 53), and activity of the enzyme is enhanced by promoters of microsomal lipid peroxidation (54). However, the molecular mechanism and identity of the lipase or lipases that mediate PL mobilization have yet to be determined.

It has been shown that increase of phospholipase A1 activity stimulates hepatic uptake of cholesterol of high density lipoprotein and induces hepatic cholesterol accumulation (55, 56). Hence, we speculate that depletion of hepatic PLs and the possible increase of phospholipase A1 activity in PPARα-deficient mice may contribute to lowering of serum cholesterol level under fasting conditions. Further experiments will be required to delineate more precisely this mechanism.

Arachidonic, eicosapentaenoic, and docosahexaenoic acids and their metabolite derivatives can function as intracellular signaling molecules, regulating gene expression via fatty acid-activated transcription factors (27, 28, 57, 58), or exerting its effects by modulating protein kinase C (59) and by calcium mobilization (60). Hence, the selective depletion of PLs and mobilization of arachidonic, eicosapentaenoic, and docosahexaenoic acids during energy deprivation in the absence of PPARα expression might modulate gene expression profiles, as well as altering membrane property, of which the long-term physiological effects have not been assessed.

In conclusion, our data show that fasting leads to a remarkable accumulation of TG but a dramatic depletion of PLs in the livers of PPARα deficient mice. These results suggest that PPARα is required for regulation of fatty acid metabolism as well as maintenance of PL homeostasis.

The authors thank the Laboratory Animal Service Unit for breeding and providing the transgenic animal, Dr. Z. Y. Chen for advice in gas chromatographic separation of fatty acids, and Ms. Frances K. I. Tong for technical assistance. This work was supported by a Strategic Research Programme grant from the Chinese University of Hong Kong (SRP9603).

REFERENCES

1. Evans, R. M. 1988. The steroid and thyroid hormone receptor superfamily. *Science.* **240:** 889–895.
2. O'Malley, B. 1990. The steroid receptor superfamily: more excitement predicted for the future. *Mol. Endocrinol.* **4:** 363–369.
3. Kliewer, S. A., B. M. Forman, B. Blumberg, E. S. Ong, U. Borgmeyer, D. J. Mangelsdorf, K. Umesono, and R. M. Evans. 1994. Differential expression and activation of a family of murine peroxisome proliferator-activated receptors. *Proc. Natl. Acad. Sci. USA.* **91:** 7355–7359.
4. Braissant, O., F. Foufelle, C. Scotto, M. Dauca, and W. Wahli. 1996. Differential expression of peroxisome proliferator-activated receptors (PPARs): tissue distribution of PPAR-α, -β, and -γ in the adult rat. *Endocrinology.* **137:** 354–366.
5. Schmidt, A., N. Endo, S. J. Rutledge, R. Vogel, D. Shinar, and G. A. Rodan. 1992. Identification of a new member of the steroid hormone receptor superfamily that is activated by a peroxisome proliferator and fatty acids. *Mol. Endocrinol.* **6:** 1634–1641.
6. Ibrahimi, A., L. Teboul, D. Gaillard, E. Z. Amri, G. Ailhaud, P. Young, M. A. Cawthorne, and P. A. Grimaldi. 1994. Evidence for a common mechanism of action for fatty acids and thiazolidinedione antidiabetic agents on gene expression in preadipose cells. *Mol. Pharmacol.* **46:** 1070–1076.
7. Greene, M. E., B. Blumberg, O. W. McBride, H. F. Yi, K. Kronquist, K. Kwan, L. Hsieh, G. Greene, and S. D. Nimer. 1995. Isolation of the human peroxisome proliferator activated receptor γ cDNA: expression in hematopoietic cells and chromosomal mapping. *Gene Expr.* **4:** 281–299.
8. Elbrecht, A., Y. Chen, C. A. Cullinan, N. Hayes, M. Leibowitz, D. E. Moller, and J. Berger. 1996. Molecular cloning, expression and characterization of human peroxisome proliferator activated receptors γ1 and γ2. *Biochem. Biophys. Res. Commun.* **224:** 431–437.
9. Chen, F., S. W. Law, and B. W. O'Malley. 1993. Identification of two mPPAR related receptors and evidence for the existence of five subfamily members. *Biochem. Biophys. Res. Commun.* **196:** 671–677.
10. Zhu, Y., K. Alvares, Q. Huang, M. S. Rao, and J. K. Reddy. 1993. Cloning of a new member of the peroxisome proliferator-activated receptor gene family from mouse liver. *J. Biol. Chem.* **268:** 26817–26820.
11. Dreyer, C., G. Krey, H. Keller, F. Givel, G. Helftenbein, and W. Wahli. 1992. Control of the peroxisomal β-oxidation pathway by a novel family of nuclear hormone receptors. *Cell.* **68:** 879–887.
12. Gottlicher, M., E. Widmark, Q. Li, and J. A. Gustafsson. 1992. Fatty acids activate a chimera of the clofibric acid-activated receptor and the glucocorticoid receptor. *Proc. Natl. Acad. Sci. USA.* **89:** 4653–4657.
13. Sher, T., H. F. Yi, O. W. McBride, and F. J. Gonzalez. 1993. cDNA cloning, chromosomal mapping, and functional characterization of the human peroxisome proliferator activated receptor. *Biochemistry.* **32:** 5598–5604.
14. Tugwood, J. D., I. Issemann, R. G. Anderson, K. R. Bundell, W. L. McPheat, and S. Green. 1992. The mouse peroxisome proliferator activated receptor recognizes a response element in the 5′ flanking sequence of the rat acyl CoA oxidase gene. *EMBO J.* **11:** 433–439.
15. Tontonoz, P., E. Hu, R. A. Graves, A. I. Budavari, and B. M. Spiegelman. 1994. mPPAR γ2: tissue-specific regulator of an adipocyte enhancer. *Genes Dev.* **8:** 1224–1234.
16. Rodriguez, J. C., G. Gil-Gomez, F. G. Hegardt, and D. Haro. 1994. Peroxisome proliferator-activated receptor mediates induction of the mitochondrial 3-hydroxy-3-methylglutaryl-CoA synthase gene by fatty acids. *J. Biol. Chem.* **269:** 18767–18772.
17. Poirier, H., I. Niot, M. C. Monnot, O. Braissant, C. Meunier-Durmort, P. Costet, T. Pineau, W. Wahli, T. M. Willson, and P. Besnard. 2001. Differential involvement of peroxisome-proliferator-activated receptors α and δ in fibrate and fatty-acid-mediated inductions of the gene encoding liver fatty-acid-binding protein in the liver and the small intestine. *Biochem. J.* **355:** 481–488.
18. Lemberger, T., B. Desvergne, and W. Wahli. 1996. Peroxisome proliferator-activated receptors: a nuclear receptor signaling pathway in lipid physiology. *Annu. Rev. Cell Dev. Biol.* **12:** 335–363.
19. Schoonjans, K., B. Staels, and J. Auwerx. 1996. The peroxisome proliferator activated receptors (PPARs) and their effects on lipid metabolism and adipocyte differentiation. *Biochim. Biophys. Acta.* **1302:** 93–109.
20. Lee, C. H., P. Olson, and R. M. Evans. 2003. Minireview: lipid metabolism, metabolic diseases, and peroxisome proliferator-activated receptors. *Endocrinology.* **144:** 2201–2207.
21. Kroetz, D. L., P. Yook, P. Costet, P. Bianchi, and T. Pineau. 1998. Peroxisome proliferator-activated receptor α controls the hepatic CYP4A induction adaptive response to starvation and diabetes. *J. Biol. Chem.* **273:** 31581–31589.

22. Kersten, S., J. Seydoux, J. M. Peters, F. J. Gonzalez, B. Desvergne, and W. Wahli. 1999. Peroxisome proliferator-activated receptor α mediates the adaptive response to fasting. *J. Clin. Invest.* **103:** 1489–1498.
23. Leone, T. C., C. J. Weinheimer, and D. P. Kelly. 1999. A critical role for the peroxisome proliferator-activated receptor α (PPARα) in the cellular fasting response: the PPARα-null mouse as a model of fatty acid oxidation disorders. *Proc. Natl. Acad. Sci. USA.* **96:** 7473–7478.
24. Hashimoto, T., W. S. Cook, C. Qi, A. V. Yeldandi, J. K. Reddy, and M. S. Rao. 2000. Defect in peroxisome proliferator-activated receptor α-inducible fatty acid oxidation determines the severity of hepatic steatosis in response to fasting. *J. Biol. Chem.* **275:** 28918–28928.
25. Le May, C., T. Pineau, K. Bigot, C. Kohl, J. Girard, and J. P. Pegorier. 2000. Reduced hepatic fatty acid oxidation in fasting PPARα null mice is due to impaired mitochondrial hydroxymethylglutaryl-CoA synthase gene expression. *FEBS Lett.* **475:** 163–166.
26. Sugden, M. C., K. Bulmer, G. F. Gibbons, B. L. Knight, and M. J. Holness. 2002. Peroxisome-proliferator-activated receptor-α (PPARα) deficiency leads to dysregulation of hepatic lipid and carbohydrate metabolism by fatty acids and insulin. *Biochem. J.* **364:** 361–368.
27. Kliewer, S. A., S. S. Sundseth, S. A. Jones, P. J. Brown, G. B. Wisely, C. S. Koble, P. Devchand, W. Wahli, T. M. Willson, J. M. Lenhard, and J. M. Lehmann. 1997. Fatty acids and eicosanoids regulate gene expression through direct interactions with peroxisome proliferator-activated receptors α and γ. *Proc. Natl. Acad. Sci. USA.* **94:** 4318–4323.
28. Forman, B. M., J. Chen, and R. M. Evans. 1997. Hypolipidemic drugs, polyunsaturated fatty acids, and eicosanoids are ligands for peroxisome proliferator-activated receptors α and δ. *Proc. Natl. Acad. Sci. USA.* **94:** 4312–4317.
29. Lee, S. S., T. Pineau, J. Drago, E. J. Lee, J. W. Owens, D. L. Kroetz, P. M. Fernandez-Salguero, H. Westphal, and F. J. Gonzalez. 1995. Targeted disruption of the α isoform of the peroxisome proliferator-activated receptor gene in mice results in abolishment of the pleiotropic effects of peroxisome proliferators. *Mol. Cell. Biol.* **15:** 3012–3022.
30. Bancroft, J. D., and H. C. Cook. 1984. Manual of Histological Techniques. Churchill Livingstone, Edinburgh. 131–132.
31. Cook, H. C. 1977. Theory and Practice of Histological Techniques. Churchill Livingstone, Edinburgh. 147–148.
32. Folch, J., M. Lees, and G. H. Sloane Stanley. 1957. A simple method for the isolation and purification of total lipids from animal tissues. *J. Biol. Chem.* **226:** 497–509.
33. Morrison, W. R., and L. M. Smith. 1964. Preparation of fatty acid methyl esters and dimethylacetals from lipids with boron fluoride-methanol. *J. Lipid Res.* **5:** 600–608.
34. Lee, Y., X. Yu, F. Gonzales, D. J. Mangelsdorf, M. Y. Wang, C. Richardson, L. A. Witters, and R. H. Unger. 2002. PPARα is necessary for the lipopenic action of hyperleptinemia on white adipose and liver tissue. *Proc. Natl. Acad. Sci. USA.* **99:** 11848–11853.
35. Hegardt, F. G. 1998. Transcriptional regulation of mitochondrial HMG-CoA synthase in the control of ketogenesis. *Biochimie.* **80:** 803–806.
36. Menahan, L. A., and K. A. Sobocinski. 1983. Comparison of carbohydrate and lipid metabolism in mice and rats during fasting. *Comp. Biochem. Physiol. B.* **74:** 859–864.
37. Reddy, J. K., S. K. Goel, M. R. Nemali, J. J. Carrino, T. G. Laffler, M. K. Reddy, S. J. Sperbeck, T. Osumi, T. Hashimoto, N. D. Lalwani, and M. S. Rao. 1986. Transcriptional regulation of peroxisomal fatty acyl-CoA oxidase and enoyl-CoA hydratase/3-hydroxyacyl-CoA dehydrogenase in rat liver by peroxisome proliferators. *Proc. Natl. Acad. Sci. USA.* **83:** 1747–1751.
38. Keller, H., C. Dreyer, J. Medin, A. Mahfoudi, K. Ozato, and W. Wahli. 1993. Fatty acids and retinoids control lipid metabolism through activation of peroxisome proliferator-activated receptor-retinoid X receptor heterodimers. *Proc. Natl. Acad. Sci. USA.* **90:** 2160–2164.
39. Lopez-Luna, P., J. Olea, and E. Herrera. 1994. Effect of starvation on lipoprotein lipase activity in different tissues during gestation in the rat. *Biochim. Biophys. Acta.* **1215:** 275–279.
40. Davis, R. A., J. R. Boogaerts, R. A. Borchardt, M. Malone-McNeal, and J. Archambault-Schexnayder. 1985. Intrahepatic assembly of very low density lipoproteins: varied synthetic response of individual apolipoproteins to fasting. *J. Biol. Chem.* **260:** 14137–14144.
41. Davis, R. A., S. M. Dluz, J. K. Leighton, and V. A. Brengaze. 1989. Increased translatable mRNA and decreased lipogenesis are responsible for the augmented secretion of lipid-deficient apolipoprotein E by hepatocytes from fasted rats. *J. Biol. Chem.* **264:** 8970–8977.
42. Chinetti, G., F. G. Gbaguidi, S. Griglio, Z. Mallat, M. Antonucci, P. Poulain, J. Chapman, J. C. Fruchart, A. Tedgui, J. Najib-Fruchart, and B. Staels. 2000. CLA-1/SR-BI is expressed in atherosclerotic lesion macrophages and regulated by activators of peroxisome proliferator-activated receptors. *Circulation.* **101:** 2411–2417.
43. Chinetti, G., S. Lestavel, V. Bocher, A. T. Remaley, B. Neve, I. P. Torra, E. Teissier, A. Minnich, M. Jaye, N. Duverger, H. B. Brewer, J. C. Fruchart, V. Clavey, and B. Staels. 2001. PPAR-α and PPAR-γ activators induce cholesterol removal from human macrophage foam cells through stimulation of the ABCA1 pathway. *Nat. Med.* **7:** 53–58.
44. Chinetti, G., S. Lestavel, J. C. Fruchart, V. Clavey, and B. Staels. 2003. Peroxisome proliferator-activated receptor α reduces cholesterol esterification in macrophages. *Circ. Res.* **92:** 212–217.
45. Gavino, V. C., and G. R. Gavino. 1992. Adipose hormone-sensitive lipase preferentially releases polyunsaturated fatty acids from triglycerides. *Lipids.* **27:** 950–954.
46. Raclot, T., and R. Groscolas. 1995. Selective mobilization of adipose tissue fatty acids during energy depletion in the rat. *J. Lipid Res.* **36:** 2164–2173.
47. Conner, W. E., D. S. Lin, and C. Colvis. 1996. Differential mobilization of fatty acids from adipose tissue. *J. Lipid Res.* **37:** 290–298.
48. Lazarow, P. B. 1978. Rat liver peroxisomes catalyze the β oxidation of fatty acids. *J. Biol. Chem.* **253:** 1522–1528.
49. Flatmark, T., A. Nilsson, J. Kvannes, T. S. Eikhom, M. H. Fukami, H. Kryvi, and E. N. Christiansen. 1988. On the mechanism of induction of the enzyme systems for peroxisomal β-oxidation of fatty acids in rat liver by diets rich in partially hydrogenated fish oil. *Biochim. Biophys. Acta.* **962:** 122–130.
50. Renaud, G., J. Marais, and R. Infante. 1980. Effect of fasting on the lipid composition and enzyme activity of rat liver plasma membranes. *Experientia.* **36:** 642–643.
51. Gasbarrini, A., A. B. Borle, H. Farghali, P. Caraceni, and D. Van Thiel. 1993. Fasting enhances the effects of anoxia on ATP, Ca^{2+} and cell injury in isolated rat hepatocytes. *Biochim. Biophys. Acta.* **1178:** 9–19.
52. Waite, M., and P. Sisson. 1973. Solubilization by heparin of the phospholipase A1 from the plasma membranes of rat liver. *J. Biol. Chem.* **248:** 7201–7206.
53. Kucera, G. L., P. J. Sisson, M. J. Thomas, and M. Waite. 1988. On the substrate specificity of rat liver phospholipase A1. *J. Biol. Chem.* **263:** 1920–1928.
54. Beckman, J. K., S. M. Borowitz, and I. M. Burr. 1987. The role of phospholipase A activity in rat liver microsomal lipid peroxidation. *J. Biol. Chem.* **262:** 1479–1484.
55. Bamberger, M., S. Lund-Katz, M. C. Phillips, and G. H. Rothblat. 1985. Mechanism of the hepatic lipase induced accumulation of high-density lipoprotein cholesterol by cells in culture. *Biochemistry.* **24:** 3693–3701.
56. Johnson, W. J., M. J. Bamberger, R. A. Latta, P. E. Rapp, M. C. Phillips, and G. H. Rothblat. 1986. The bidirectional flux of cholesterol between cells and lipoproteins: effects of phospholipid depletion of high density lipoprotein. *J. Biol. Chem.* **261:** 5766–5776.
57. Duplus, E., M. Glorian, and C. Forest. 2000. Fatty acid regulation of gene transcription. *J. Biol. Chem.* **275:** 30749–30752.
58. Mater, M. K., A. P. Thelen, and D. B. Jump. 1999. Arachidonic acid and PGE2 regulation of hepatic lipogenic gene expression. *J. Lipid Res.* **40:** 1045–1052.
59. O'Flaherty, J. T., D. P. Jacobson, J. F. Redman, and A. G. Rossi. 1990. Translocation of protein kinase C in human polymorphonuclear neutrophils: regulation by cytosolic Ca^{2+}-independent and Ca^{2+}-dependent mechanisms. *J. Biol. Chem.* **265:** 9146–9152.
60. Sergeeva, M., M. Strokin, H. Wang, J. J. Ubl, and G. Reiser. 2002. Arachidonic acid and docosahexaenoic acid suppress thrombin-evoked Ca^{2+} response in rat astrocytes by endogenous arachidonic acid liberation. *J. Neurochem.* **82:** 1252–1261.